Limits on $K_L^0 \to \pi^0 e^+ e^-$ and $K_L^0 \to e^+ e^-$

E. Jastrzembski, R. C. Larsen, L. B. Leipuner, and W. M. Morse
Department of Physics, Brookhaven National Laboratory, Upton, New York 11973

H. B. Greenlee, H. Kasha, E. B. Mannelli, M. Mannelli, K. E. Ohl, S. F. Schaffner, and M. P. Schmidt
Department of Physics, Yale University, New Haven, Connecticut 06511
(Received 24 June 1988)

We report on a search for the flavor-changing neutral-current decays $K_L^0 \to \pi^0 e^+ e^-$ and $K_L^0 \to e^+ e^-$. Limits obtained for these processes are $B(K_L^0 \to \pi^0 e^+ e^-) < 3.2\times10^{-7}$ and $B(K_L^0 \to e^+ e^-) < 1.2\times10^{-9}$.

PACS numbers: 13.20.Eb, 11.30.Hv, 12.15.Mm

The decays $K_L^0 \to \pi^0 e^+ e^-$ and $K_L^0 \to e^+ e^-$ occur as a consequence of strangeness changing neutral currents and are highly suppressed in the standard model. Moreover, the decay $K_L^0 \to \pi^0 e^+ e^-$ through one photon exchange is a *CP*-violating process. Decays to $\pi^0 e^+ e^-$ can proceed through vector or scalar currents, while decays to $e^+ e^-$ are mediated by axial vector or pseudoscalar currents.

The decay $K^+ \to \pi^+ e^+ e^-$ is known to occur[1] with a branching ratio of $(2.7\pm0.5)\times10^{-7}$. Theoretical estimates[2] of the decay rate for the *CP*-conserving decay $K_S^0 \to \pi^0 e^+ e^-$ range from $\frac{1}{10}$ of the rate for $K^+ \to \pi^+ e^+ e^-$ to 2.5 times that rate while the rate for similar $K_L^0 \to \pi^0 e^+ e^-$ decays is expected to be reduced by the factor ϵ^2 in the absence of any direct *CP*-violating amplitude. Theoretical estimates[2] of the transition $K_L^0 \to \pi^0 e^+ e^-$ range from 2×10^{-12} to 3×10^{-11}. The decay $K_L^0 \to \pi^0 e^+ e^-$ is then an excellent window to search for light scalar particles than couple to $e^+ e^-$. Furthermore, some nonstandard models of *CP*-invariance violation[3] predict branching ratios higher than 3×10^{-11}. The present 90% confidence-level limit[4] for this decay is $B(K_L^0 \to \pi^0 e^+ e^-) < 2.3\times10^{-6}$.

The decay $K_L^0 \to e^+ e^-$ is suppressed in the standard model with respect to the observed rare decay $K_L^0 \to \mu^+ \mu^-$ because of the small value of m_e/m_k. The unitarity limit for $K_L^0 \to e^+ e^-$ is $B(K_L^0 \to e^+ e^-) > 2.5\times10^{-12}$. This decay is then particularly sensitive to new interactions proceeding through pseudoscalar currents. The present limit[5] is $B(K_L^0 \to e^+ e^-) < 4.5\times10^{-9}$.

The data for this study come from an experiment, optimized to search for the decay $K_L^0 \to \mu^\pm e^\mp$, conducted at the Brookhaven Alternating Gradient Synchrotron (AGS). The diagram of Fig. 1 shows a schematic representation of the experimental apparatus. A neutral beam, produced in the forward direction by the interaction of 24-GeV protons on a copper target, passed 7.47 m through a vacuum and an 8-T-m clearing field, into a 2.87-m-long decay region. γ rays from the target were attenuated by a 2.5-cm lead beam plug. The momenta of the charged particles from K decays were then determined by a magnetic spectrometer made up of two upstream sets of minidrift chambers with maximum drift distance of 3 mm (labeled A and B), a magnet with a field integral of $\Delta p_t = 220$ MeV/c, and two downstream minidrift chambers (labeled C and D). The geometrical acceptance was 3.5% for $K_L^0 \to e^+ e^-$ and 0.024% for $K_L^0 \to \pi^0 e^+ e^-$.

The electrons were identified by a 3-m-long atmospheric pressure hydrogen Cherenkov counter. Pions with energies less than 8 GeV were not registered by the Cherenekov counter. The efficiency of the Cherenkov counter was 93% for inbending electrons and 83% for outbending electrons. The electron energies were measured in a lead-glass array consisting of 244 blocks of Schott F2 glass with dimensions of $6.35\times6.35\times46$ cm^3. The glass blocks were arranged in a 1×1 m^2 array with a central 12.7×38 cm^2 hole to pass the neutral beam. Custom-built analog-to-digital-converter modules were used to integrate the charge from the lead-glass counters. The signals were integrated for 120 nsec. An

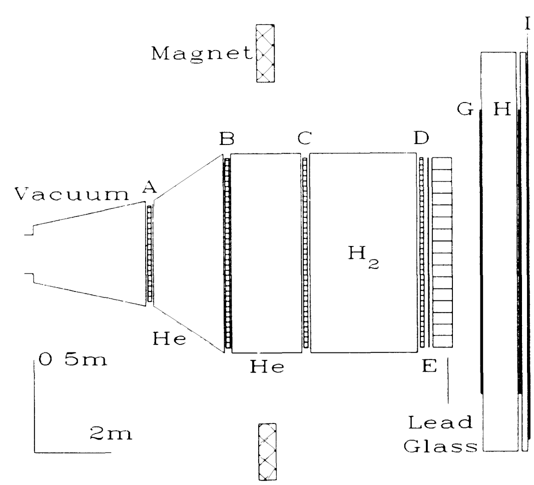

FIG. 1. Plan view of the E780 detector. Note the different horizontal and vertical scales.

"in-time bit" was set if a leading edge above an effective threshold of 500 MeV occurred within ±5 nsec of the trigger. We accepted typically 8×10^{11} protons per AGS pulse, which generated approximately 10^7 counts/(m^2 sec) in the detector.

Four trigger types were collected: μe, ee, $\mu\mu$, and $\pi\pi$. All triggers required drift-chamber hits on the left and on the right of the neutral beam in the bend-view drift chambers. As defined by the hardware trigger, electrons were particles that triggered the Cherenkov counter and deposited at least 1.2 GeV in the glass array; particles which penetrated a 1.05-m steel filter were defined as muons; those particles that did not activate the μ or e triggers, but penetrated the glass array, but not the steel filter, were classified as pions. The $\pi\pi$ trigger was prescaled by a factor of 128. A Fastbus processor aborted events which did not have A, B, and C drift-chamber hits compatible with two tracks in the bend view which originated in the decay volume. However, no on-line cuts were made to reject three-body decays. The data-acquisition live time was typically 90%.

The ee triggers largely derive K_{e3} decays such that the pion energy is above the Cherenkov threshold. The energy deposited in the lead glass for electrons from the K_{e3} decays was compared with the momentum determined in the magnetic spectrometer to provide an accurate off-line calibration of the lead glass. The lead-glass energy resolution was determined to be $\sigma/E=11\%/\sqrt{E}$ (E in GeV). The resolution was measured to be $7\%/\sqrt{E}$ when the glass was purchased. We attribute the difference to radiation damage. Most of the blocks appear noticeably yellow compared to new lead glass. The lead-glass position resolution was measured to be ±6 mm.

Measurements of the decay $K_L^0\to\pi^0\pi^+\pi^-$ serve to determine a normalization for the $K_L^0\to\pi^0e^+e^-$ decays as well as providing a useful measure of mass resolutions for the topologically similar $\pi^0e^+e^-$ final states. The charged tracks were required to pass requirements on track quality and distance of closest approach at the vertex. Events were rejected if there were more than two tracks[6] pointing to the vertex. All events were required to have at least two γ clusters in the lead glass besides the two clusters associated with the charged tracks. The γ clusters were required to be in a fiducial region which excluded the blocks around the beam hole. Only those γ clusters were selected such that greater than 1 GeV was deposited in the cluster and the in-time bit was activated. Figure 2(a) shows a histogram of the measured $\gamma\gamma$ invariant mass for such events. For events with more than two γ clusters, all $\gamma\gamma$ invariant mass combinations are shown. Only events with exactly one $\gamma\gamma$ combination within 30 MeV/c^2 of the π^0 mass were selected. If the invariant mass of the $\gamma\gamma$ set within 30 MeV/c^2 of the π^0 mass is constrained to the π^0 mass, the K mass is determined to an uncertainty of $\sigma=3.7$ MeV/c^2. With this result as a normalization, the mass uncertainty for the final-state $\pi^0e^+e^-$ was calculated to be $\sigma=4.4$ MeV/c^2.

The events are also constrained by the requirement that they point back to the target. For otherwise acceptable $\pi^0\pi^+\pi^-$ events, $\sigma(\theta)\approx1$ mrad, where θ is the angle between the line from target to the decay point and the total momentum vector. We require that $\pi^+\pi^-\pi^0$ events be within 12.5 MeV/c^2 of the K mass and have $\theta^2<10$ mrad^2. The $\pi^+\pi^-\pi^0$ effective mass and θ^2 distributions are shown in Figs. 2(b) and 2(c), respectively. These distributions are especially clean. No corrections have been made for background under the peaks.

The resolution for e^+e^- decays is determined from the kinematically similar $K_L^0\to\pi^+\pi^-$ sample. Figure 3(a) shows the $\pi^+\pi^-$ effective mass for inbending events. The distribution in θ^2 is shown in Fig. 3(b). The mass resolution is 2.3 MeV/c^2 for inbending events and

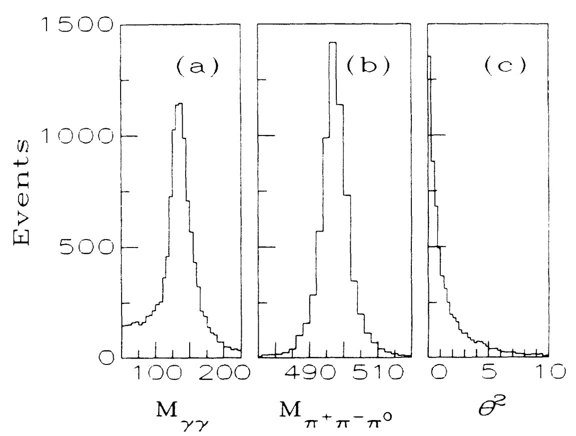

FIG. 2. Distributions of (a) $\gamma\gamma$ effective mass (MeV/c^2), (b) $\pi^+\pi^-\pi^0$ effective mass (MeV/c^2) for events with $\theta^2<10$ mrad^2, and (c) the square of the target reconstruction angle (mrad^2) for events within 12.5 MeV/c^2 of the K mass.

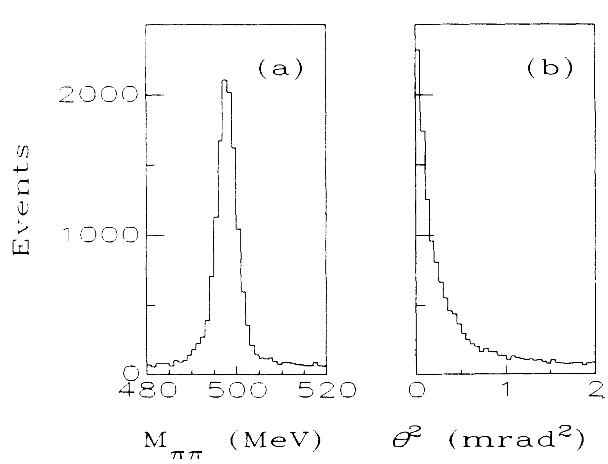

FIG. 3. Distributions of (a) the $\pi^+\pi^-$ invariant mass for inbending events with $\theta^2<1.5$ mrad^2 and (b) the square of the target reconstruction angle for events within 3σ of the K mass.

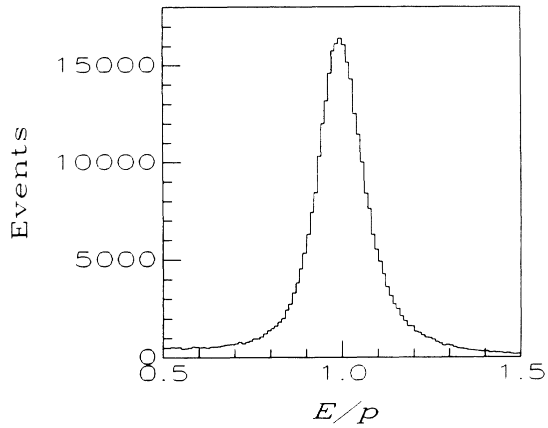

FIG. 4. Distribution of energy measured in the lead glass divided by momentum measured in the magnetic spectrometer for electrons from K_{e3} decays.

4.0 MeV/c^2 for outbending events. The resolution in θ is 0.33 mrad for both event samples. We require that the $\pi^+\pi^-$ events be within 3σ of the K mass and have $\theta^2 < 1.5$ mrad^2. However, radiative effects[7] are important for decays to $\pi^0e^+e^-$ and e^+e^-. For example, 15% of $K_L^0 \to e^+e^-$ decays will have an e^+e^- effective mass more than 20 MeV/c^2 below the K mass.

Electron identification was established off-line by use of the lead-glass information. The momentum measured in the magnetic spectrometer was required to be close to the energy measured in the lead-glass array. The distribution in E/p for K_{e3} events from μe and ee triggers is shown in Fig. 4. The tail at large E/p is due to accidental overlap at high rates and is not seen in low-intensity runs. We require $E/p > 0.75$ for electrons. Furthermore, the electron momentum was required to be below the pion Cherenkov threshold of 8 GeV/c for the $\pi^0e^+e^-$ search and the e^+e^- effective mass was required to be greater than 150 MeV/c^2 to reject π^0 Dalitz decays. The momentum asymmetry $A = (p_{max} - p_{min})/(p_{max} + p_{min})$ was required to be less than 0.6 for the e^+e^- search. From Monte Carlo calculations, it was determined that $>97\%$ of e^+e^- decays satisfy the momentum asymmetry constraint.

Figure 5 shows a plot of the e^+e^- effective mass versus θ^2 for e^+e^- triggers which satisfy the above criteria. We find no events consistent with $K_L^0 \to e^+e^-$. The nearest event with an acceptable θ^2 is 25 MeV/c^2 below the K mass. The events below the K mass are consistent with the Monte Carlo calculations of K_{e3} events with the pion misidentified as an electron. The normalization for $K_L^0 \to e^+e^-$ is determined by the number of observed $K_L^0 \to \pi^+\pi^-$ decays. A correction of 15% was applied to account for background contributions in mass and θ^2. The background-subtracted data were then fitted as functions of K energy and decay position to determine the K_S^0 contamination. It was determined that effectively 78% of the $\pi\pi$ decays were due to K_L^0. Then, by use of the known $\pi\pi$ branching ratio and the ratio of ee to $\pi\pi$ acceptances as determined by Monte Carlo calculations, the single event sensitivity to $K_L^0 \to e^+e^-$ was determined to be 7.2×10^{-10}. We then determine the 90% confidence-level limit $B(K_L^0 \to e^+e^-) < 1.6\times10^{-9}$. Combination of this result with our earlier limit[5] gives a final limit $B(K_L^0 \to e^+e^-) < 1.2\times10^{-9}$.

A plot of $m(\pi^0e^+e^-)$ vs θ^2 is shown in Fig. 6. There were no $\pi^0e^+e^-$ candidate events consistent with pointing back to the target. Only one of the events in the plot survives a more stringent lead-glass cut of $0.85 < E/p < 1.25$. The acceptance of the experiment to $\pi^0e^+e^-$ was calculated by Monte Carlo methods as a function of the e^+e^- effective mass. The dileptons were generated isotropically in their rest frame. The normalization for $\pi^0e^+e^-$ was determined through an accounting of the topologically similar decay $K_L^0 \to \pi^0\pi^+\pi^-$. The 90% confidence-level limits on $K_L^0 \to \pi^0e^+e^-$ are shown as a function of the e^+e^- effective mass in Fig. 7.

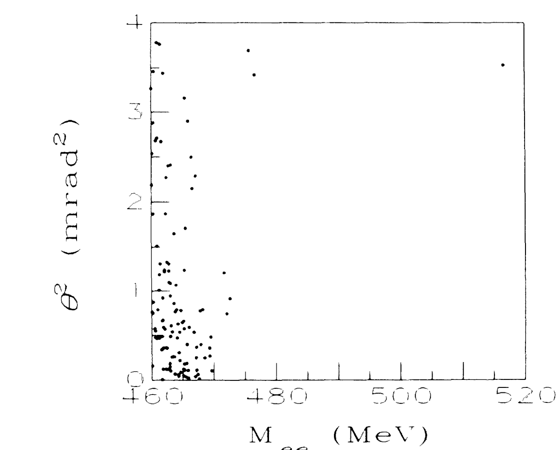

FIG. 5. Scatter plot of the e^+e^- effective mass vs the square of the target reconstruction angle.

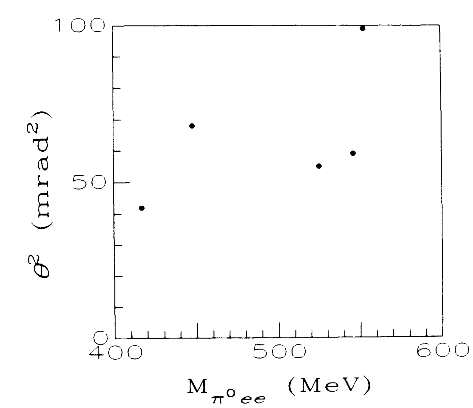

FIG. 6. Scatter plot of the $\pi^0e^+e^-$ effective mass vs the square of the target reconstruction angle.

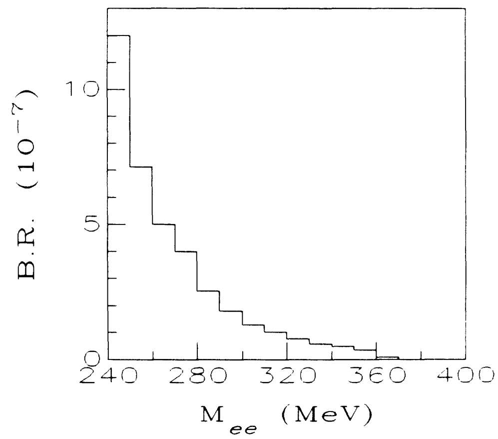

FIG. 7. 90% confidence-level limits on $K_L^0 \rightarrow \pi^0 e^+ e^-$ as a function of the e^+e^- effective mass.

For a population of events distributed uniformly in the Dalitz plot, the 90% confidence limit is $B(K_L^0 \rightarrow \pi^0 e^+ e^-) < 3.6 \times 10^{-7}$.

During an earlier run, approximately $\frac{1}{3}$ of the data were taken without on-line cuts to reject three-body K decays. The analog-to-digital-converter in-time bit was not implemented for that run. There was one event consistent with pointing back to the target ($\theta^2 = 0.7 \times 10^{-6}$). However, the $\pi^0 e^+ e^-$ effective mass was only 481 MeV/c^2. Furthermore, this event, which had additional hits in the first two drift chambers, was consistent with the decay $K_L^0 \rightarrow \pi^0 \pi^0$ with both π^0's undergoing Dalitz decay.[8] A cut was applied to the data to reject events with extra track stubs.[6] This cut rejected about 1.5% of the normalization events. After application of this cut, there were no events left in the region shown in Fig. 6. If we combine the results from both runs, the 90% confidence-level limit is $B(K_L^0 \rightarrow \pi^0 e^+ e^-) < 3.2 \times 10^{-7}$.

We gratefully acknowledge the contributions of R. K. Adair who worked on the earlier stages of the experiment. We also thank Michael Lenz and Joseph Yelk who made technical contributions to the experiment. This research is supported by the U.S. Department of Energy under Contracts No. DE-AC02-76CH00016 and No. DE-AC02-76ER03075. Additional support for one of us (M.P.S.) is provided by the Alfred P. Sloan Foundation.

[1]P. Bloch *et al.*, Phys. Lett. **56B**, 201 (1975); N. J. Baker *et al.*, Phys. Rev. Lett. **59**, 2832 (1987).

[2]J. F. Donoghue, B. R. Holstein, and G. Valencia, Phys. Rev. D **35**, 2769 (1987); G. Ecker, A. Pich, and E. deRafael, Nucl. Phys. **B291**, 692 (1987), and **B303**, 665 (1988).

[3]L. J. Hall and L. J. Randall, Nucl. Phys. **B274**, 157 (1986).

[4]A. S. Carroll *et al.*, Phys. Rev. Lett. **44**, 525 (1980).

[5]H. B. Greenlee *et al.*, Phys. Rev. Lett. **60**, 893 (1988).

[6]An event is rejected if there is an extra space point in the A drift chamber within 6 mm of a line extrapolated from the decay vertex to an extra space point in the B drift chamber.

[7]L. Bergström, Z. Phys. C **20**, 135 (1983).

[8]M. Mannelli *et al.*, in Proceedings of the Twenty-Third Recontres de Moriond, Les Arcs, France, 6–13 March 1988 (to be published). The additional hits in the A and B drift chambers were not consistent with originating at the decay vertex within the accuracy of the drift-chamber measurements. However, if their momenta were about 170 and 200 MeV/c, the trajectories were consistent with originating at the vertex when the effects of multiple scattering in the vacuum window and magnetic curvature in the small fringe field between the A and B chambers is taken into consideration. These particles would have curled in the spectrometer field and would not have been observed in the C and D drift chambers. The effective-mass combinations are then $m(\gamma_1 e_1^+ e_1^-) = 125$ MeV/c^2, $m(\gamma_2 e_2^+ e_2^-) = 145$ MeV/c^2, and $m(\gamma_1 \gamma_2 e_1^+ e_2^+ e_1^- e_2^-) = 497$ MeV/c^2, consistent with the π^0 and K^0 masses, respectively. The lead-glass E/p for the high-energy positron and electron were 1.01 and 1.05, respectively. We calculate the probability of observing a $\pi^0\pi^0$ decay with both π^0's undergoing Dalitz decay such that a $\gamma\gamma e^+ e^-$ effective-mass combination is 480 MeV/c^2 or higher is less than 1%.